RESEARCH PAPER

Acta Neurobiol Exp 2022, 82: 263–272
DOI: 10.55782/ane-2022-025

Comprehensive analysis of lncRNA-miRNA-mRNA regulatory networks for Alzheimer's disease

Fenghua Li[1]*, Zaihong Lin[2], Gengsheng Tian[3]

[1] Department of Neurology, Qiqihar First Hospital, Qiqihar City, China,
[2] Department of Neurology, The Third Affiliated Hospital of Qiqihar Medical College, Qiqihar City, China,
[3] General Surgery, Lindian County Hospital of Daqing City, Daqing City, China,
** Email: lifenghua00001@163.com*

Alzheimer's disease (AD) is a progressive and irreversible neurodegenerative disease, associated with a decreased cognitive function and severe behavioral abnormalities. This study aimed to explore mechanisms of development and progression of AD. Comprehensive analysis of GSE16759 was performed to identify the differentially expressed lncRNAs (DElncRNAs), miRNAs (DEmiRNAs), and mRNAs (DEmRNAs). The differentially expressed RNAs (DERs) were used for the subsequent analysis, including module genes analysis, pathway enrichment analysis, and interaction network analysis. Finally, an AD-associated network consisting of lncRNA-miRNA-mRNA-pathway was constructed. A total of 431 DEmRNAs, 35 DElncRNAs, and 103 DEmiRNAs between the AD group and the normal control group were identified. DEmRNAs were significantly enriched in 13 pathways, such as focal adhesion, endocytosis, and mTOR signaling pathway. Three modules significantly related to AD were finally screened. The AD-associated network was constructed, including 2 lncRNAs (*A2M-AS1* and *ZNF571-AS1*), 1 miRNA (*hsa-miR-206*), 2 mRNAs (*NOTCH3* and *JAG1*), and 2 pathways (notch signaling pathway and endocrine resistance). *A2M-AS1*, *ZNF571-AS1*, *hsa-miR-206*, *NOTCH3* and *JAG1* may be involved in the mechanisms of AD through notch signaling pathway and endocrine resistance.

Key words: Alzheimer's disease, interaction network analysis, notch signaling pathway

INTRODUCTION

Alzheimer's disease (AD) is the commonest cause of dementia affecting older people (Birks and Harvey, 2018). AD is a progressive and irreversible neurodegenerative disease, associated with a decreased cognitive function and severe behavioral abnormalities (Song et al., 2017; Wang et al., 2017). AD may occur due to apoptosis of neurons in the brain, and especially memory-related areas including glutamatergic neurons in the entorhinal cortex and the CA1 field of the hippocampus, as well as cholinergic neurons in the basal forebrain. Despite decades of study, effective treatments for AD are lacking (Lee et al., 2018). Improved understanding of the underlying mechanisms of AD may eventually identify novel therapeutic targets for patients. Early diagnosis is important to improve prognosis and reduce mortality. With the rapid development of molecular biological detection technology, molecular markers of AD have been paid more and more attention to find the key molecular targets for targeted treatment, and ultimately improve the survival rate of AD patients (Caroli and Frisoni, 2010; Liang et al., 2010). Generally, ncRNAs are categorized into two classes according to their size. The first class of ncRNAs is short ncRNAs including microRNAs (miRNAs), PIWI-interacting RNAs, small interfering RNA, small nuclear ribonucleic acid, transcription initiation RNAs, small nucleolar RNAs, promoter-associated small RNAs, and TSS-associated RNAs (Cortini et al., 2019; Maniati et al., 2019). The second class

Received 17 February 2022, accepted 13 June 2022

of ncRNAs is long noncoding RNAs (lncRNAs), which have a length of more than 200 bp and less than 100 kb. It is proposed that ncRNAs can be used as novel diagnostic and prognostic biomarkers or therapeutic targets of neurodegenerative disease. Accumulating evidence has demonstrated that miRNAs and lncRNAs play a crucial role in various biological processes such as brain development, maturation, differentiation, neuronal cell specification, neurogenesis, myelination, neurotransmission, and synaptic plasticity (Salta and De Strooper, 2012).

The traditional pathological examination is not enough to predict the treatment outcome, so it is of great significance to study its pathogenesis from the perspective of molecular biology. Gene expression profile is effective for the classification and prognosis of tumor patients. This paper comprehensively analyzed the gene expression profiles, and screened the important genes related to AD. In this study, comprehensive analysis of GSE16759 was performed to identify the differentially expressed lncRNAs (DE lncRNAs), miRNAs (DEmiRNAs), and mRNAs (DEmRNAs). The differentially expressed RNAs (DERs) were used for the subsequent analysis, including pathway enrichment analysis and interaction network analysis to explore mechanisms of the development and progression of AD.

METHODS

Data preprocessing

The dataset GSE16759 produced by Nunez-Iglesias et al. (2010) of the parietal areas of the cerebral cortex of AD patients (n=4) and normal control persons (n=4) were downloaded from Gene Expression Omnibus (GEO) (Barrett et al., 2007), and the platform was Affymetrix Human Genome U133 Plus 2.0 Array and Human 0.9 K miRNA-940-v1.0. The data were preprocessed, including background correction, quantile normalization, and probe summarization, using Oligo package (version 1.34.0) in R language (Irizarry et al., 2003) and limma (version 3.10.3) package (Kerr, 2003).

Identification of DERs and pathway enrichment analysis

We re-annotated mRNAs and lncRNAs in the expression profile through HUGO Gene Nomenclature Committee (HGNC) (http://www.genenames.org/), including 4338 lncRNAs and 19218 protein coding genes (Yates et al., 2017). The data were calculated by limma (version 3.34.0) package (Ritchie et al., 2015) to identify DERs between the AD group and the normal control group with FDR < 0.05 and |log2FC| > 0.5 as the cut-off. The heatmap of DERs was plotted using pheatmap package (version 1.0.8) in R language (Bhattacharjee et al., 2002; Wang et al., 2014). Pathway enrichment analysis of mRNAs was performed using the software KOBAS 3.0, and the significant enrichment pathways with FDR < 0.05 were selected (Wu et al., 2006).

Module genes analysis

Gene modules were generated by weighted gene co-expression network analyses (WGCNA) through WGCNA package (version 1.61) in R language (Chen et al., 2012; Langfelder and Horvath, 2008) with the numbers of module RNAs > 30 and cutHeight = 0.995 as the cut-off. Combined with the clinical information, the relationships between modules and clinical traits were measured, and modules significantly positively related to AD were selected with $p<0.05$ as the threshold. DERs in these modules were used for the subsequent analysis.

Analysis of ceRNA network

DIANA-LncBase version 2 (http://carolina.imis.athena-innovation.gr/diana_tools/web/index.php), is a database that records the lncRNA-miRNA relationship pairs. We used DIANA-LncBase version 2 to select the lncRNA-miRNA relationship pairs, and the pairs with the miRNA target gene score (miTG-score) > 0.8 and the opposite expression tendency of lncRNAs and miRNAs were screened. The network of lncRNA-miRNA relationship pairs was constructed using Cytoscape software (Shannon et al., 2003). The database starBase Version 2.0 (http://starbase.sysu.edu.cn/), including miRanda, PITA, Pictar, RNA22, and Targetscan, was used to predict the target genes of miRNAs (Li et al., 2014), and the pairs with opposite expression tendency of miRNAs and genes were selected. The networks of miRNA-target genes relationship pairs and lncRNA-miRNA-mRNA relationship pairs were constructed using Cytoscape software. Pathway enrichment analysis of mRNAs in the network was performed using the software KOBAS 3.0, and the significant enrichment pathways with FDR<0.05 were selected. The database Comparative Toxicogenomics Database 2019 update (http://ctd.mdibl.org/) was used to search the KEGG pathways related to AD (Davis et al., 2018), and the network consisting of lncRNA-miRNA-mRNA-pathway relationship pairs was constructed using Cytoscape software.

RESULTS

Analysis of DERs

A total of 1708 lncRNAs, 476 miRNAs and 17387 mRNAs were re-annotated using HUGO Gene Nomenclature Committee (HGNC) (additional file 1). A total of 431 DEmRNAs (154 up-regulated and 277 down-regulated genes), 35 DElncRNAs (27 up-regulated and 8 down-regulated lncRNAs), and 103 DEmiRNAs (64 up-regulated and 39 down-regulated miRNAs) between the AD group and the normal control group were identified, and the distribution of DERs was shown in Fig. 1. DEmRNAs were significantly enriched in focal

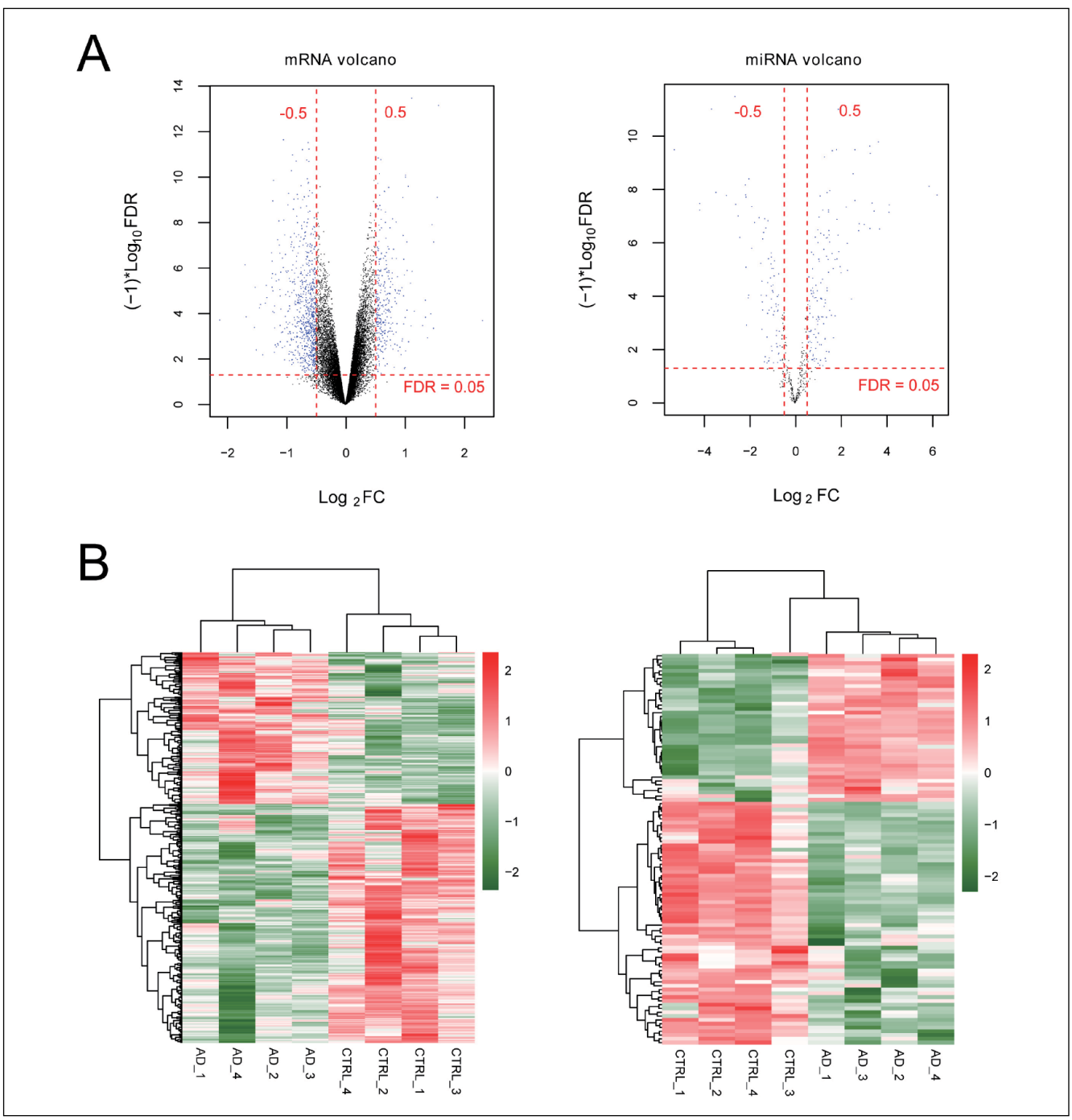

Fig. 1. The results of DERs. (A) The volcano of DEmRNAs (genes and lncRNAs) and DEmiRNAs between the AD group and the normal control group. (B) The heatmap of DEmRNAs (genes and lncRNAs) and DEmiRNAs between the AD group and the normal control group.

adhesion, endocytosis, mTOR signaling pathway, MAPK signaling pathway, endocrine resistance, rap1 signaling pathway, estrogen signaling pathway, ras signaling pathway, TNF signaling pathway, axon guidance, pathways in cancer, Parkinson's disease and AD (Fig. 2 and additional file 2).

Screening stable modules based on WGCNA

Eight gene modules were generated by WGCNA (Fig. 3B). The blue, green and red modules were significantly positively related to AD (Fig. 3C). RNAs in the three modules were shown in additional file 3, and a total of 175 RNAs were used for further analysis.

The interaction network analysis

We constructed an interaction network for DElncRNAs and DEmiRNAs, and the result was shown in Fig. 4. The network included 22 nodes (10 down-regulated miRNAs and 12 up-regulated lncRNAs; *A2M-AS1*, *FAM13A-AS1*, *FAM157A*, *FTX*, *KIAA1614-AS1*, *LINC00342*, *LINC00620*, *LINC00852*, *ST7-AS1*, *TNRC6C-AS1*, *VLDLR-AS1*, *ZNF571-AS1*, *hsa-miR-206*,

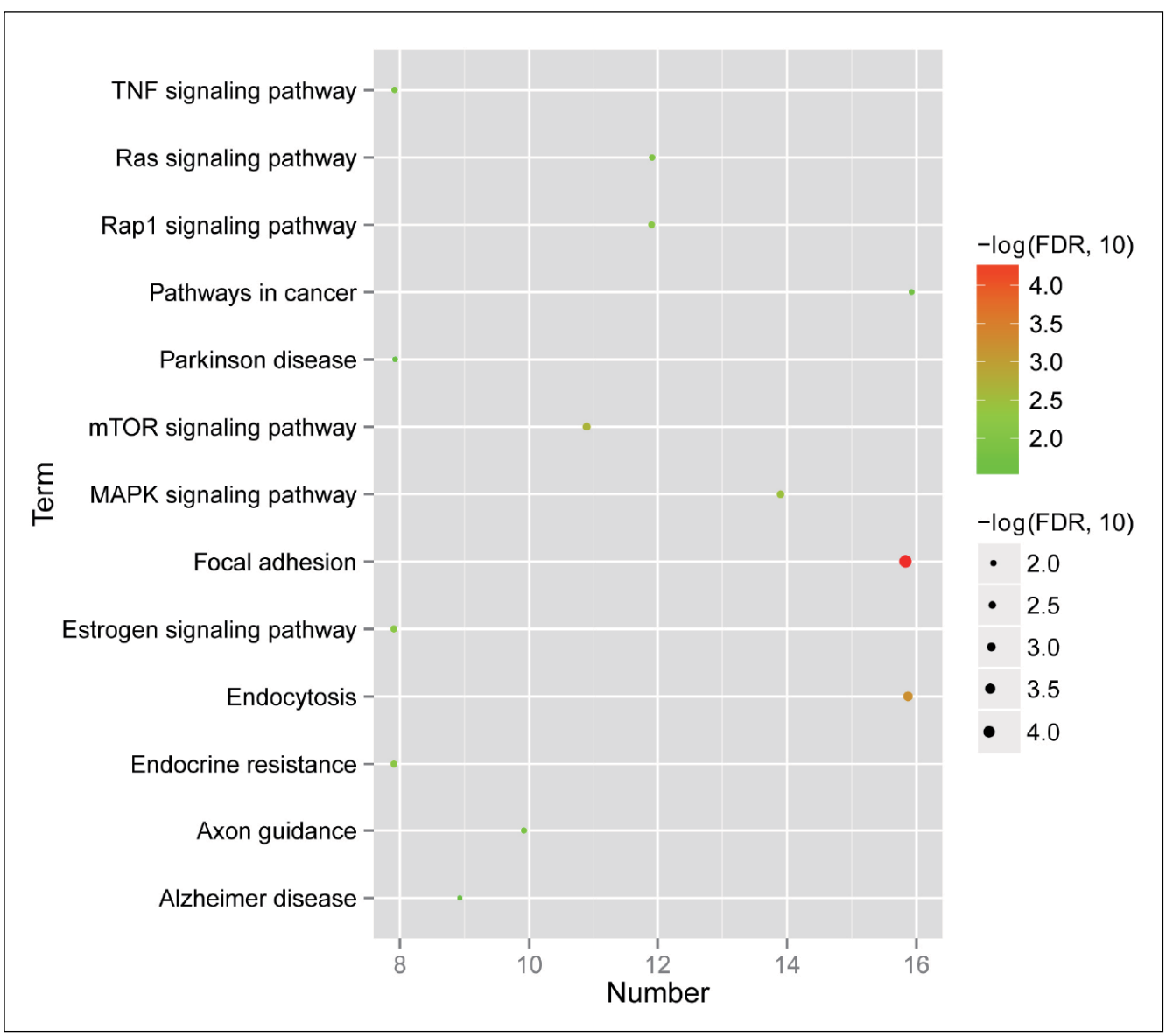

Fig. 2. The enrichment pathways of DEGs. The horizontal axis represented the number of genes; the vertical axis represented the KEGG pathways, and the size and color of the dots represented -log10(FDR).

hsa-miR-617, *hsa-miR-765*, *hsa-miR-133b*, *hsa-miR-198*, *hsa-miR-638*, *hsa-miR-498*, *hsa-miR-409-3p*, *hsa-miR-575* and *hsa-miR-346*). The interaction network of DEmiRNAs and DEGs was shown in Fig. 5, and the network included 30 nodes (6 down-regulated miRNAs and 24 up-regulated mRNAs; *hsa-miR-346*, *hsa-miR-409-3p*, *hsa-miR-498*, *hsa-miR-198*, *hsa-miR-206*, *hsa-miR-133b*, *EPHA2*, *COLEC12*, *CSRNP1*, *CAV1*, *NACA*, *UBE2D3*, *SLC12A7*, *ARHGAP18*, *SLC12A2*, *TGFB1I1*, *TFPI*, *GCH1*, *DLG1*, *PTPN14*, *KDELR2*, *MLLT3*, *HNRNPL*, *JAG1*, *NOTCH3*, *LZTS2*, *COL5A3*, *RNF41*, *TES* and *ABCA2*). The interaction network of DElncRNAs, DEmiRNAs and DEGs was shown in Fig. 6, and the network included 46 nodes (12 lncRNAs, 10 miRNAs and 24 mRNAs). mRNAs in the lncRNA-miRNA-mRNA network were significantly enriched in notch signaling pathway (*NOTCH3* and *JAG1*), endocrine resistance (*NOTCH3* and *JAG1*) and folate biosynthesis (*GCH1*). CTD database showed that there were 207 pathways related to AD (additional file 4). Combined with the results of the lncRNA-miRNA-mRNA network, notch signaling

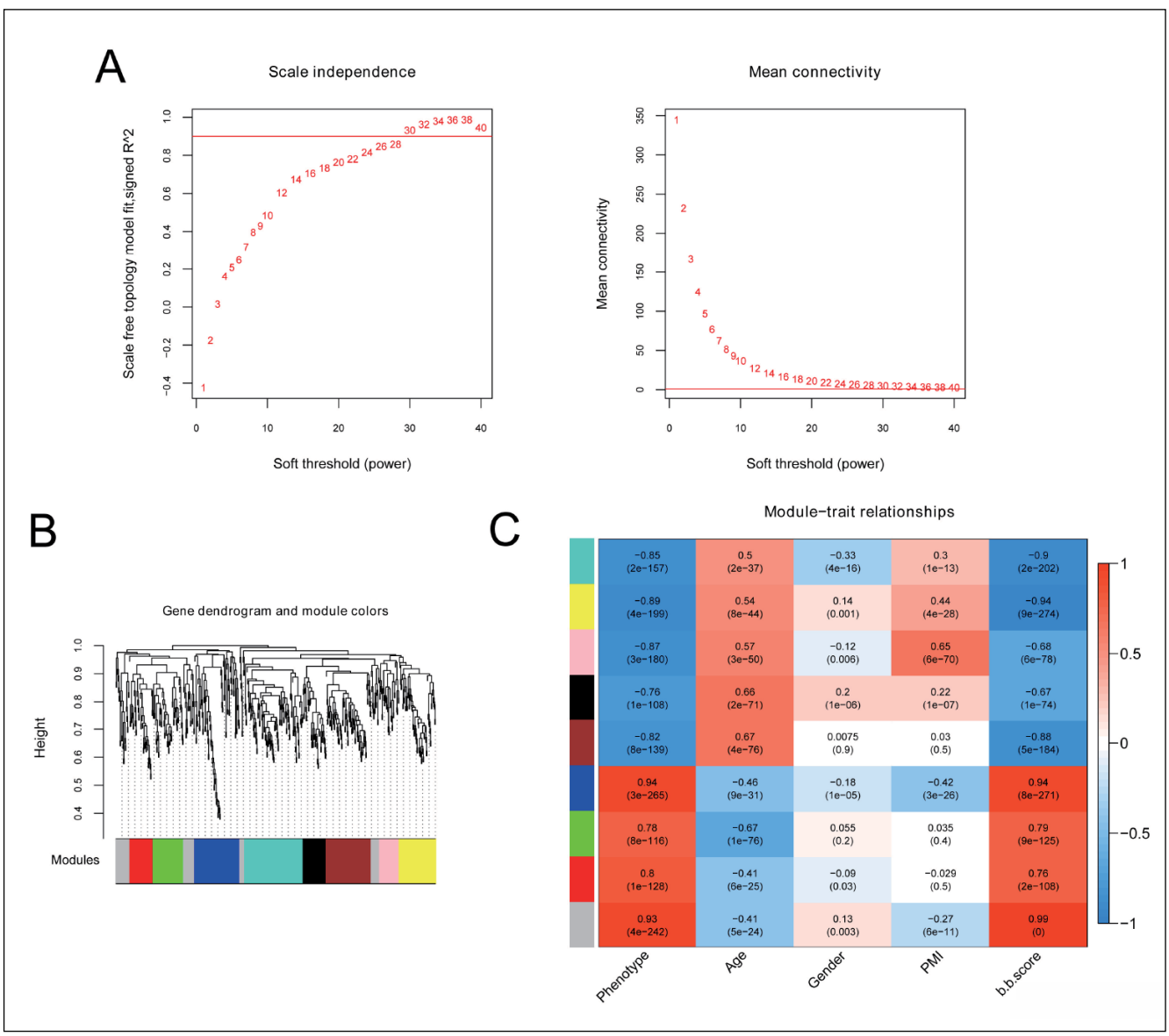

Fig. 3. The module results based on WGCNA. (A-left) power selection diagram of adjacency matrix weight parameter. The horizontal axis represented the weight parameter power, and the vertical axis represented the square of the log(k) and log(p(k)) correlation coefficients in the corresponding network. (A-right) schematic diagram of RNA average connectivity under different power parameters. (B) tree diagrams of the modules, and each color represented a different module. (C) the correlation heatmap of module-trait. The trait data was obtained from the original publication of GSE16759 and attached as additional file 6, phenotype represented disease or control, and PMI represented postmortem interval.

pathway and endocrine resistance were screened, and the AD-associated network consisting of lncRNA-miRNA-mRNA-pathway was constructed in this study (Fig. S1).

DISCUSSION

AD is a progressive and irreversible neurodegenerative disease, associated with a decreased cognitive function and severe behavioral abnormalities. Increasing data have demonstrated that ncRNAs such as miRNAs and lncRNAs are associated with the pathogenesis of AD. In this study, comprehensive analysis of GSE16759 was performed to identify the DElncRNAs, DEmiRNAs, and DEmRNAs. The DERs were used for the subsequent analysis, including pathway enrichment analysis and interaction network analysis to explore mechanisms of the development and progression of AD. A total of 431 DEmRNAs were significantly enriched in focal adhesion, endocytosis, mTOR signaling pathway, MAPK signaling pathway, endocrine resistance, rap1 signaling pathway, estrogen signaling pathway, ras signaling pathway, TNF signaling pathway, axon guidance, pathways in cancer, Parkinson's disease and Alzheimer's disease. lncRNA-miRNA and miRNA-mRNA pairs with negative correlation were utilized for the construction of lncRNA-miRNA-mRNA network. Positive correlations between levels of miRNAs and their target mRNAs were observed by Nunez-Iglesias et al(Nunez-Iglesias-et al., 2010), meanwhile, they also found a few negatively correlated miRNA-mRNA pairs, and the relative abundance of different correlations drived the average. We selected the negatively correlated pairs since most of regulations in the ceRNA regulatory network exhibited inhibitory. Combined with the results of the lncRNA-miRNA-mRNA network, notch signaling pathway and endocrine resistance were screened, and the AD-associated network was constructed, including 2 lncRNAs (*A2M-AS1* and *ZNF571-AS1*), 1 miRNA (*hsa-miR-206*), 2 mRNAs (*NOTCH3* and *JAG1*), and 2 pathways (notch signaling pathway and endocrine resistance). *NOTCH3*, *JAG1*, *A2M-AS1* and *ZNF571-AS1* were significantly up-regulated, while *hsa-miR-206* was obvious-

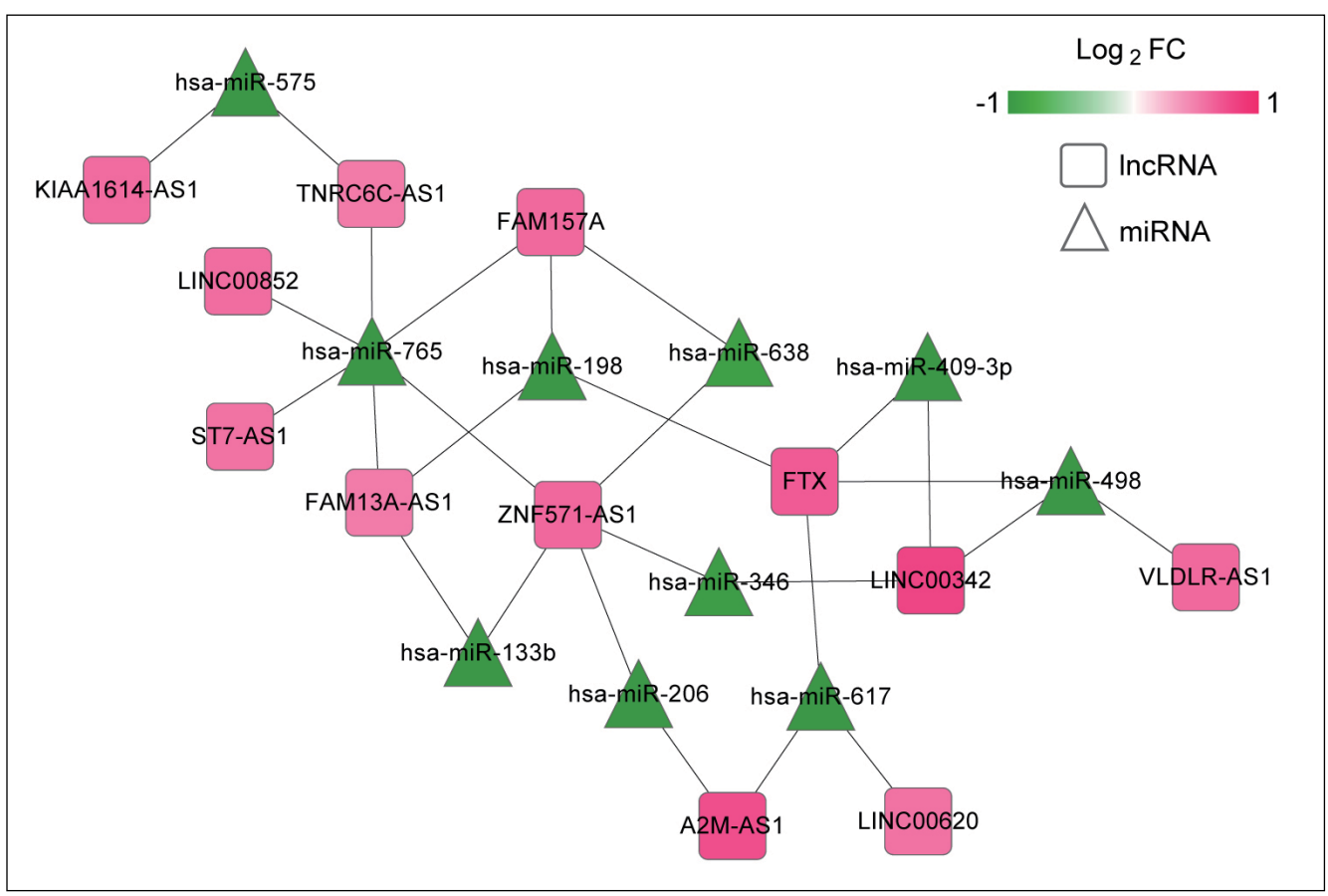

Fig. 4. The interaction network of DElncRNAs and DEmiRNAs. Square and triangle respectively represented lncRNA and miRNA, and the change of color from green to red indicated a significant down-regulation to up-regulation expression change.

ly down-regulated, and most of these RNAs exhibited similar expression patterns in other research (Fig. S2 and additional file 5).

Alpha-2-macroglobulin (*A2M*) is a molecule generally associated with inflammation, and chronic inflammation is associated with ageing and cancer (Thieme et al., 2015; Šunderić et al., 2019). *A2M* was a biomarker of neuronal injury in AD and a network of nine genes co-expressed with *A2M* in the brain was identified (Varma et al., 2017; Seddighi et al., 2018). *miR-206*, which suppresses the expression of brain-derived neurotrophic factor, is known to be elevated in the brains of AD patients (Moon et al., 2016). The increased serum *miR-206* level might be a potential predictor of conversion from amnestic mild cognitive impairment (aMCI) to AD (Xie et al., 2017). Circulating *miR-206* and *miR-132* as novel miRNAs upregulated in mild cognitive impairment (MCI) patient were potential biomarkers for diagnosis of MCI (Xie et al., 2015). Brain-derived neurotrophic factor (*BDNF*) is required for efficient skeletal-muscle regeneration and perturbing its expression causes ab-

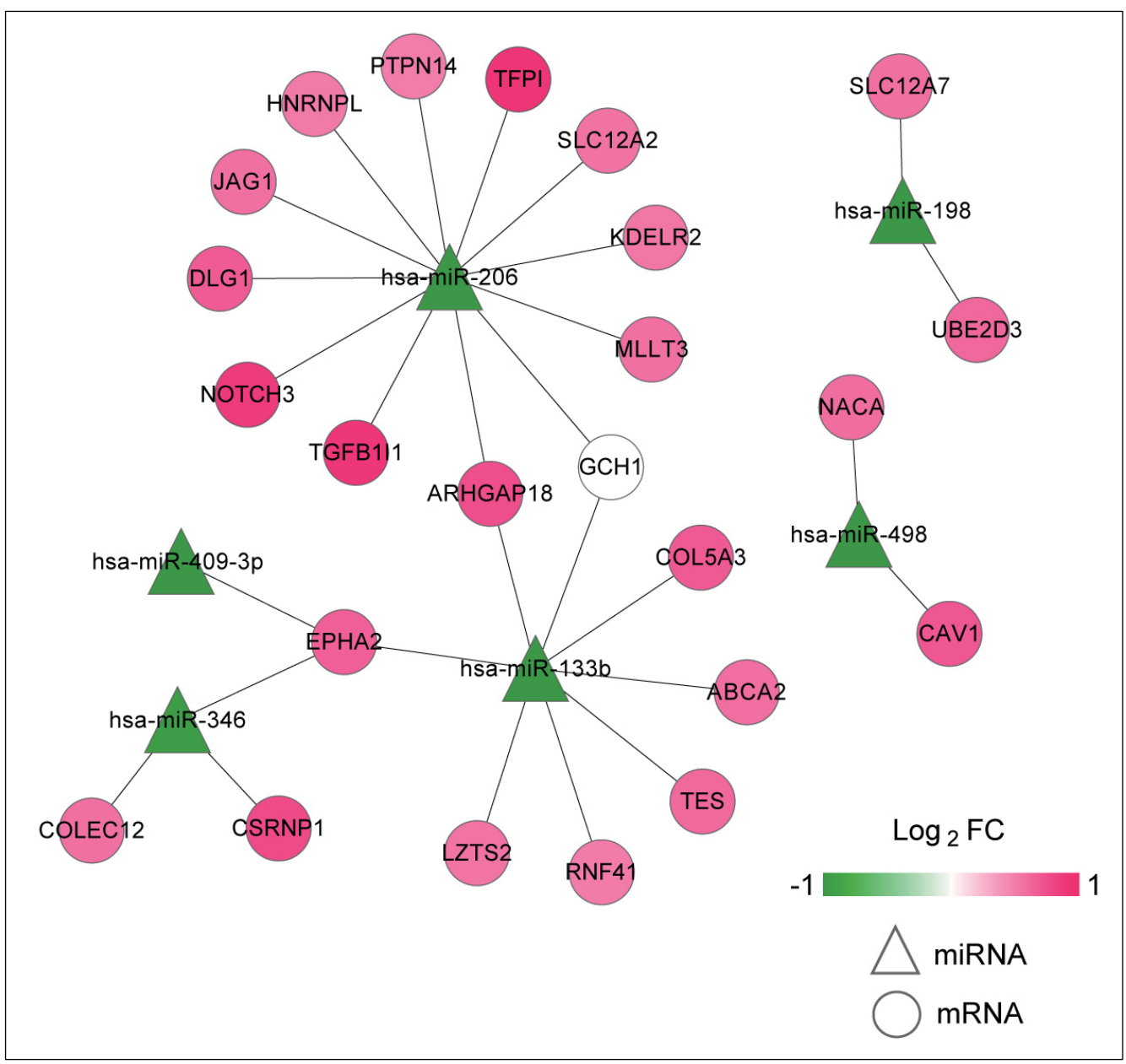

Fig. 5. The interaction network of DEmiRNAs and target genes. Circular and triangle respectively represented mRNAs and miRNAs, and the change of color from green to red indicated a significant down-regulation to up-regulation expression change.

normalities in the proliferation and differentiation of skeletal muscle cells, and *miR-206* might play a role in regulating retrograde signaling of *BDNF* at the neuromuscular junction (Miura et al., 2012). The increased *miR-206* down-regulated the expression of *BDNF* (Tian et al., 2014). Furthermore, intranasally administered *miR-206* also reached the brain and increased *BDNF* levels and memory function in AD mice (Lee et al., 2012). Cerebral autosomal-dominant arteriopathy with subcortical infarcts and leukoencephalopathy (*CADASIL*) pathophysiology was associated with hypomorphic *Notch 3* function in vascular smooth muscle cells and implicated the accumulation of clusterin and collagen 18 α1/endostatin in brain vessel pathology (Joutel et al., 1996, Thomas et al., 2000). *MRK-003* inhibited *Notch3* signaling, reduced tumor cell proliferation, inhibited serum independence, and induced apoptosis (Konishi et al., 2007). Hypomorphic *Notch 3* alleles linked *Notch* signaling to ischemic cerebral small-vessel disease (Arboleda-Velasquez et al., 2011). *Notch3* was identified as a target of *miR-206* that was involved in the negative regulation of *Notch3* anti-apoptosis signaling. Through its inhibition of *Notch3* signaling, *miR-206* could active cellular apoptosis and suppress tumor growth (Song et al., 2009). Physiological functions of β-Site Amyloid Precursor Protein Cleaving Enzyme 1(*BACE1*) may limit its use as a therapeutic target for AD (Barão et al., 2016). *BACE1* can effectively shed the membrane-anchored signaling molecule Jagged 1 (*Jag1*). Although *Jag1* shares a high degree of homology with *Jag2* in the ectodomain region, *BACE1* fails to cleave *Jag2* effectively, indicating a selective cleavage of *Jag1*. Abolished cleavage of *Jag1* in *BACE1*-null mice leads to enhanced astrogenesis and, concomitantly, reduced neurogenesis. This characterization provides biochemical evidence that the *Jag1-Notch* pathway is under the control of *BACE1* activity. *Jag1* is a ligand of the *Notch* pathway and a target of *miR-206*, and *miR-206* overexpression inhibited *Jag1*. Through ligand binding to receptors, *Notch* signaling is activated to initiate an intercellular communication system(Kopan and Ilagan, 2009). Decreased *Jag1* inactivated the *Notch* pathway, while downregulation of *miR-206* could re-activate the abrogated *Notch* signaling (Hu et al., 2021).

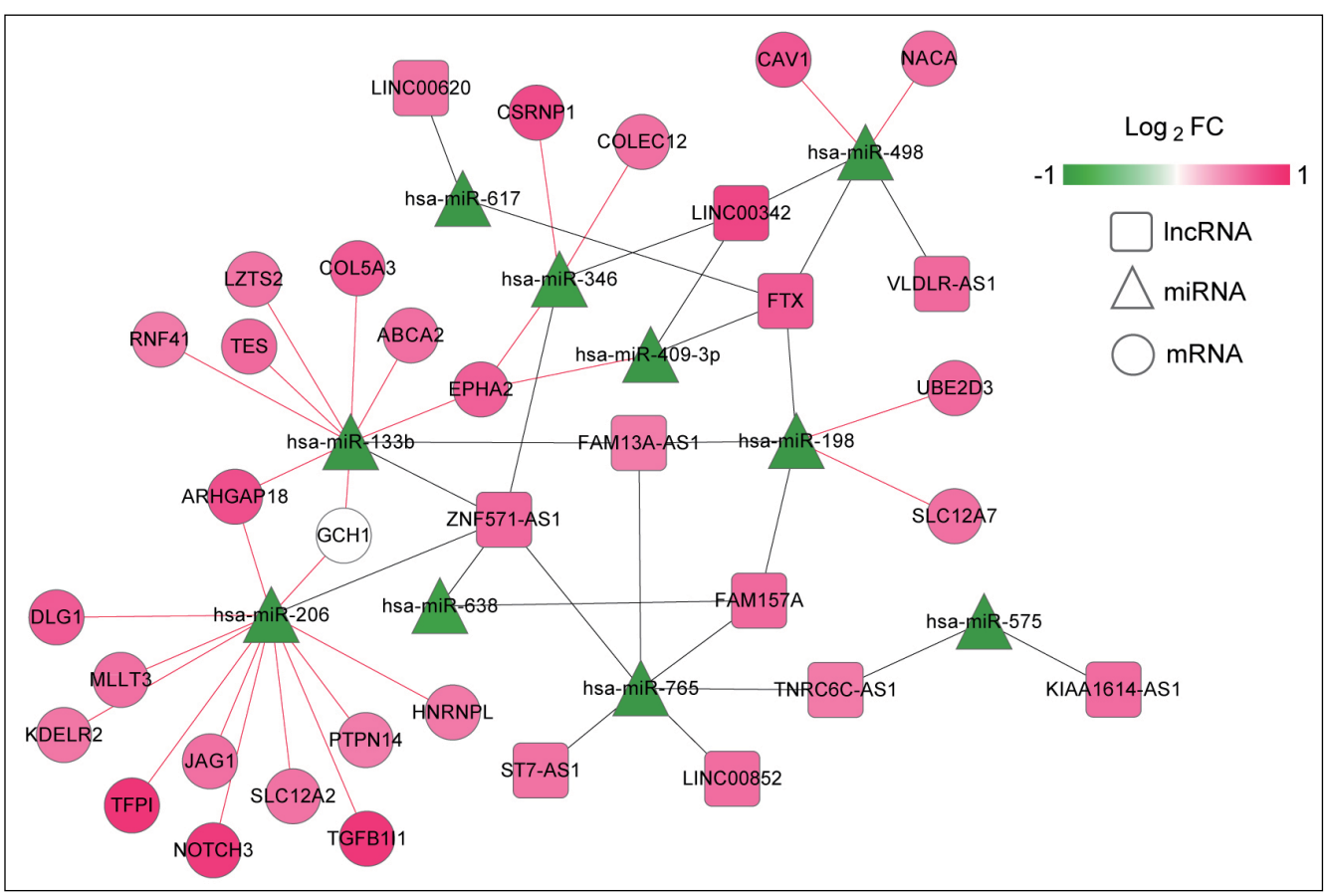

Fig. 6. The interaction network of DElncRNAs, DEmiRNAs and target genes. Square, triangle, and circular respectively represented lncRNAs, miRNAs and target genes, and the change of color from green to red indicated a significant down-regulation to up-regulation expression change.

CONCLUSION

In conclusion, an AD-associated network consisting of lncRNA-miRNA-mRNA-pathway was constructed, implying that *A2M-AS1*, *ZNF571-AS1*, *hsa-miR-206*, *NOTCH3*, and *JAG1* may be involved in the mechanisms of AD through notch signaling pathway and endocrine resistance.

REFERENCES

Arboleda-Velasquez JF, Manent J, Lee JH, Tikka S, Ospina C, Vanderburg CR, et al. (2011) Hypomorphic Notch 3 alleles link Notch signaling to ischemic cerebral small-vessel disease. Proc Natl Acad Sci USA 108: E128–135.

Barão S, Moechars D, Lichtenthaler SF, De Strooper B (2016) BACE1 physiological functions may limit its use as therapeutic target for Alzheimer's disease. Trends Neurosci 39: 158–169.

Barrett T, Troup DB, Wilhite SE, Ledoux P, Rudnev D, Evangelista C, et al. (2007) NCBI GEO: mining tens of millions of expression profiles-database and tools update. Nucleic Acids Res 35: D760–765.

Bhattacharjee R, Bramel J, Hash T, Kolesnikova-Allen A, Khairwal S (2002) Assessment of genetic diversity within and between pearl millet landraces. Theor Appl Genet 105: 666–673.

Birks JS, Harvey RJ (2018) Donepezil for dementia due to Alzheimer's disease. Cochrane DB Syst Rev 6: Cd001190.

Caroli A, Frisoni GB (2010) The dynamics of Alzheimer's disease biomarkers in the Alzheimer's Disease Neuroimaging Initiative cohort. Neurobiol Aging 31: 1263–1274.

Chen R, Mias GI, Li-Pook-Than J, Jiang L, Lam HY, Chen R, et al. (2012) Personal omics profiling reveals dynamic molecular and medical phenotypes. Cell 148: 1293–1307.

Cortini F, Roma F, Villa C (2019) Emerging roles of long non-coding RNAs in the pathogenesis of Alzheimer's disease. Ageing Res Rev 50: 19–26.

Davis AP, Wiegers TC, Wiegers J, Johnson RJ, Sciaky D, Grondin CJ, et al. (2018) Chemical-induced phenotypes at CTD help inform the predisease state and construct adverse outcome pathways. Toxicol Sci 165: 145–156.

Hu G, Ma J, Zhang J, Chen Y, Liu H, Huang Y, et al. (2021) Hypoxia-induced lncHILAR promotes renal cancer metastasis via ceRNA for the miR-613/206/1–1-3p/Jagged-1/Notch/CXCR4 signaling pathway. Mol Ther 29: 2979–2994.

Irizarry RA, Hobbs B, Collin F, Beazer-Barclay YD, Antonellis KJ, Scherf U, et al. (2003) Exploration, normalization, and summaries of high density oligonucleotide array probe level data. Biostatistics 4: 249–264.

Joutel A, Corpechot C, Ducros A, Vahedi K, Chabriat H, Mouton P, et al. (1996) Notch3 mutations in CADASIL, a hereditary adult-onset condition causing stroke and dementia. Nature 383: 707–710.

Kerr MK (2003) Linear models for microarray data analysis: hidden similarities and differences. J Comput Biol 10: 891–901.

Konishi J, Kawaguchi KS, Vo H, Haruki N, Gonzalez A, Carbone DP, et al. (2007) Gamma-secretase inhibitor prevents Notch3 activation and reduces proliferation in human lung cancers. Cancer Res 67: 8051–8057.

Kopan R, Ilagan MXG (2009) The canonical Notch signaling pathway: unfolding the activation mechanism. Cell 137: 216–233.

Langfelder P, Horvath S (2008) WGCNA: an R package for weighted correlation network analysis. BMC Bioinformatics 9: 559.

Lee J, Kim Y, Liu T, Hwang YJ, Hyeon SJ, Im H, et al. (2018) SIRT3 deregulation is linked to mitochondrial dysfunction in Alzheimer's disease. Aging Cell 17: e12679.

Lee ST, Chu K, Jung KH, Kim JH, Huh JY, Yoon H, et al. (2012) miR-206 regulates brain-derived neurotrophic factor in Alzheimer disease model. Ann Neurol 72: 269–277.

Li JH, Liu S, Zhou H, Qu LH, Yang JH (2014) starBase v2.0: decoding miRNA-ceRNA, miRNA-ncRNA and protein-RNA interaction networks from large-scale CLIP-Seq data. Nucleic Acids Res 42: D92–97.

Liang KY, Mintun MA, Fagan AM, Goate AM, Bugg JM, Holtzman DM, et al. (2010) Exercise and Alzheimer's disease biomarkers in cognitively normal older adults. Ann Neurol 68: 311–318.

Maniati MS, Maniati M, Yousefi T, Ahmadi-Ahangar A, Tehrani SS (2019) New insights into the role of microRNAs and long noncoding RNAs in most common neurodegenerative diseases. J Cell Biochem 120: 8908–8918.

Miura P, Amirouche A, Clow C, Bélanger G, Jasmin BJ (2012) Brain-derived neurotrophic factor expression is repressed during myogenic differentiation by miR-206. J Neurochem 120: 230–238.

Moon J, Lee ST, Kong IG, Byun JI, Sunwoo JS, Shin JW, et al. (2016) Early diagnosis of Alzheimer's disease from elevated olfactory mucosal miR-206 level. Sci Rep 6: 20364.

Nunez-Iglesias J, Liu CC, Morgan TE, Finch CE, Zhou XJ (2010) Joint genome-wide profiling of miRNA and mRNA expression in Alzheimer's disease cortex reveals altered miRNA regulation. PLoS One 5: e8898.

Ritchie ME, Phipson B, Wu D, Hu Y, Law CW, Shi W, et al. (2015) limma powers differential expression analyses for RNA-sequencing and microarray studies. Nucleic Acids Res 43: e47.

Salta E, De Strooper B (2012) Non-coding RNAs with essential roles in neurodegenerative disorders. Lancet Neurol 11: 189–200.

Seddighi S, Varma VR, An Y, Varma S, Beason-Held LL, Tanaka T, et al. (2018) SPARCL1 accelerates symptom onset in Alzheimer's disease and influences brain structure and function during aging. J Alzheimers 61: 401–414.

Shannon P, Markiel A, Ozier O, Baliga NS, Wang JT, Ramage D, et al. (2003) Cytoscape: a software environment for integrated models of biomolecular interaction networks. Genome Res 13: 2498–2504.

Song G, Zhang Y, Wang L (2009) MicroRNA-206 targets notch3, activates apoptosis, and inhibits tumor cell migration and focus formation. J Biol Chem 284: 31921–31927.

Song L, Li X, Bai XX, Gao J, Wang CY (2017) Calycosin improves cognitive function in a transgenic mouse model of Alzheimer's disease by activating the protein kinase C pathway. Neural Regen Res 12: 1870–1876.

Šunderić M, Križáková M, Malenković V, Ćujić D, Katrlík J, Nedić O (2019) Changes due to ageing in the glycan structure of alpha-2-macroglobulin and its reactivity with ligands. Protein J 38: 23–29.

Thieme R, Kurz S, Kolb M, Debebe T, Holtze S, Morhart M, et al. (2015) Analysis of alpha-2 macroglobulin from the long-lived and cancer-resistant naked mole-rat and human plasma. PloS One 10: e0130470.

Thomas NJ, Morris CM, Scaravilli F, Johansson J, Rossor M, De Lange R, et al. (2000) Hereditary vascular dementia linked to notch 3 mutations. CADASIL in British families. Ann NY Acad Sci 903: 293–298.

Tian N, Cao Z, Zhang Y (2014) MiR-206 decreases brain-derived neurotrophic factor levels in a transgenic mouse model of Alzheimer's disease. Neurosci Bull 30: 191–197.

Varma VR, Varma S, An Y, Hohman TJ, Seddighi S, Casanova R, et al. (2017) Alpha-2 macroglobulin in Alzheimer's disease: a marker of neuronal injury through the RCAN1 pathway. Mol Psychiatr 22: 13–23.

Wang J, Guo Z, Fu Y, Wu Z, Huang C, Zheng C, et al. (2017) Weak-binding molecules are not drugs?-toward a systematic strategy for finding effective weak-binding drugs. Brief Bioinform 18: 321–332.

Wang L, Cao C, Ma Q, Zeng Q, Wang H, Cheng Z, et al. (2014) RNA-seq analyses of multiple meristems of soybean: novel and alternative transcripts, evolutionary and functional implications. BMC Plant Biol 14: 169.

Wu J, Mao X, Cai T, Luo J, Wei L (2006) KOBAS server: a web-based platform for automated annotation and pathway identification. Nucleic Acids Res 34: W720–724.

Xie B, Liu Z, Jiang L, Liu W, Song M, Zhang Q, et al. (2017) Increased serum miR-206 level predicts conversion from amnestic mild cognitive impairment to Alzheimer's disease: a 5-year follow-up study. J Alzheimers 55: 509–520.

Xie B, Zhou H, Zhang R, Song M, Yu L, Wang L, et al. (2015) Serum miR-206 and miR-132 as potential circulating biomarkers for mild cognitive impairment. J Alzheimers 45: 721–731.

Yates B, Braschi B, Gray KA, Seal RL, Tweedie S, Bruford EA (2017) Genenames.org: the HGNC and VGNC resources in 2017. Nucleic Acids Res 45: D619–625.

SUPPLEMENTARY MATERIALS

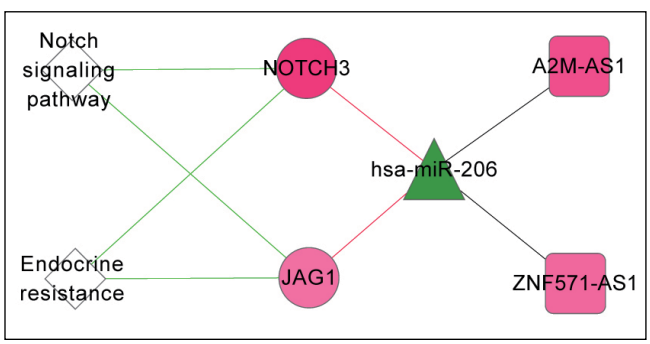

Fig. S1. The interaction network of DElncRNAs, DEmiRNAs, target genes and pathway. Square, triangle, circular and rhombus respectively represented lncRNAs, miRNAs, target genes, and pathways, and the change of color from green to red indicated a significant down-regulation to up-regulation expression change.

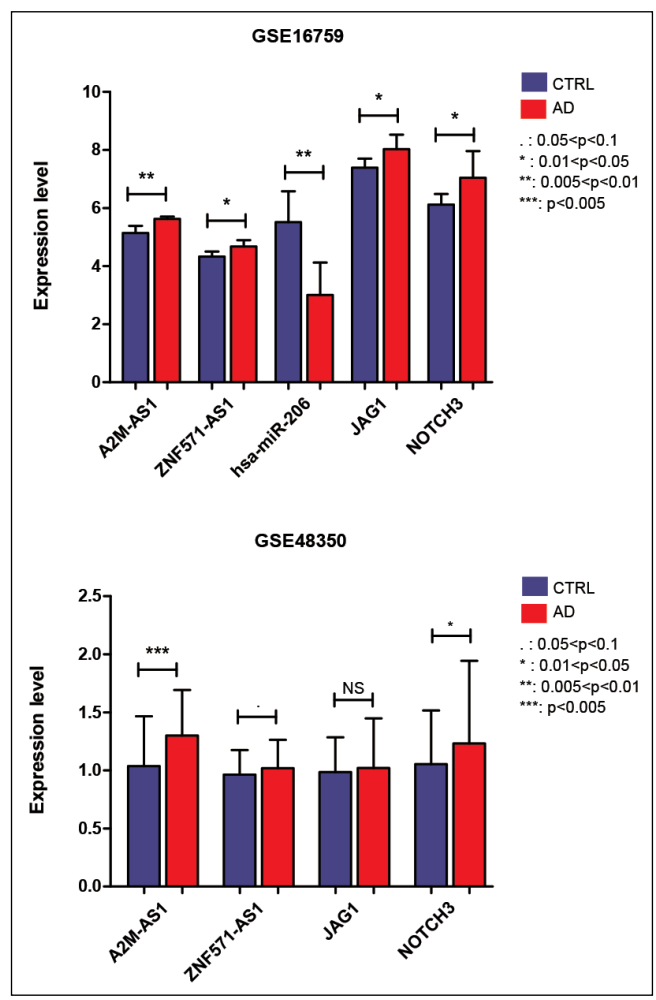

Fig. S2. The expression patterns of *A2M-AS1*, *ZNF571-AS1*, *hsa-mir-206*, *JAG1* and *NOTCH3* in GSE16759 and another AD-associated dataset GSE48350.